Improved Structural Mapping and Conductive Targeting Delivered by a new 2.5D AEM Inversion Solver

Rod Paterson *
Intrepid Geophysics
110/3 Male St., Brighton VIC
rod@intrepid-geophysics.com

Jovan Silic
Jovan Silic and Associates
Melbourne
jsilic@bigpond.com

Des FitzGerald
Intrepid Geophysics
110/3 Male St., Brighton VIC
des@intrepid-geophysics.com

SUMMARY

The advantages of 2.5D (2D geology, 3D source) airborne electromagnetic inversion in 3D geological mapping applications and the identification of conductive drilling targets compared to the more commonly used CDI transforms or simple 1D inversions are demonstrated using examples from different geological settings.

The 2.5D inversion application used in this work and described in Silic et al, 2015 is a substantially changed version of ArjunAir, Wilson et al., 2006, a product of CSIRO/AMIRA project P223F. The changes include a new forward model algorithm and a new inversion solver. The application enables the accurate simulation of 3D source excitation for full domain models inclusive of topography, non-conforming boundaries and very high resistivity contrasts. Solution is accurate for a geoelectrical cross-section which is relatively constant along a strike length that exceeds the AEM system footprint.

The major innovation includes a new inversion solver with adaptive regularisation which allows the incorporation of a misfit to the reference model and the model smoothness function. The regularisation parameter is chosen automatically and changed adaptively at each iteration, as the model, the sensitivity and the roughness matrices are changing, Silic et al, 2015.

Memory usage has been dramatically reduced and provides a usage estimate prior to execution. For speed the software has been parallelised using Intel MPI and can be used on standard computing hardware or computing clusters. Data from survey lines with lengths exceeding 30 kilometres can be inverted on high end laptop computers. The integrated software design allows the user to prepare a full survey inversion then execute this simply in a batch process. The user can visualise inversion progress at any time during process execution.

We allow flexibility in the selection of components and in the estimation of noise. A non-specialist can obtain a high value result from our 2.5D AEM inversion in terms of it achieving a more realistic geological section.

We show inversion examples from groundwater, minerals (VMS) and geological mapping AEM surveys projects and compare the results with known geology and drilling. We demonstrate the much improved mapping and target definition delivered by this inversion method when compared with the other more common transforms or inversion methods used on these projects.

Key words: inversion, electromagnetic, geology, mapping, drilling

INTRODUCTION

The advantages of 2.5D (2D geology, 3D source) airborne electromagnetic inversion in 3D geological mapping and in the identification of conductive drilling targets are demonstrated using examples from four different geological settings. The inversion results are compared with known geology and drill hole data and also with the CDI transforms, 1D and 3D inversions used on these projects.

The 2.5D inversion application used in this work is a substantially rewritten version of ArjunAir, Wilson et al., 2006 a product of CSIRO/AMIRA project P223F. This inversion application includes a new forward model algorithm and a new 2.5D inversion solver with adaptive regularisation which allows the incorporation of a misfit to the reference model and the model smoothness function. The regularisation parameter is chosen automatically and changed adaptively at each iteration, as the model, the sensitivity and the roughness matrices are changing, Silic et al, 2015.

We optionally allow a starting or reference geology/resistivity model to influence the inversion instead of a simple halfspace. The inversion application is incorporated within 3D geological modelling software with an intelligent graphical user interface allowing simple integration of this process.

The application has been re-engineered to reduce memory and increase performance by use of the INTEL Pardiso solver, INTEL MPI parallelisation and optimisation of the sensitivity matrix. This enables data from survey lines with lengths exceeding 30 kilometres to be inverted on a high end laptop computer. An I7 class computer with 16 to 32GB RAM will manage a full 2.5D

inversion of most AEM surveys. The integrated software design allows the user to prepare a full survey inversion then execute this simply in a batch process. The user can visualise inversion progress at any time during process execution.

We show inversion examples from groundwater, minerals (VMS) and geological mapping AEM surveys projects and compare the results with known geology and drilling. We demonstrate the much improved 3D mapping and target definition delivered by this inversion method when compared with the other more common transforms or inversion methods used on these projects.

The project examples include data from TEMPEST, VTEM™ *max* and *HELITEM*® time domain and RESOLVE frequency domain systems.

We show the ability of this inversion application to accurately resolve the 3D geology and conductivity distribution and in some cases provide sufficient detail to allow direct target drilling to be designed without the need for detailing using ground EM. Resolution of geology to depths of >1km are demonstrated where the system power and conductivity distribution allow.

Improved geological resolution is clearly apparent when compared with the other transform and inversion methods used on these projects. Subtle late time features that are not easily identified visually will be recognised by this 2.5D inversion method.

METHOD

Airborne EM data from each of the selected projects has been inverted using the 2.5D inversion application described in the summary above. The work flow is as follows:

1. Build a system file to describe the AEM system waveform and measurement time gates
2. Create a 3D GeoModeller project to cover the survey area extents
3. Load the survey database and generate a 2D section for each flight line
4. Define system measurement units and geometry in the setup interface
5. Estimate system noise from the observed data using a low signal area of the survey where possible.
6. Choose the finite element mesh geometry for the 2.5D inversion i.e. define the cell resolution
7. Select the 2.5D inversion parameters, Survey sample interval, RSVT start value, number of iterations etc. The inversion parameters have some automatic checks to ensure that invalid selections are adjusted to ensure a stable inversion
8. Choose the starting model and resistivity (default is halfspace) or select a reference model if a priori info available.
9. Choose the maximum number of iterations and misfit criteria. Software contains some smart adaptive get out criteria to ensure the inversion does not over/under fit the data.
10. Choose the number of CPU's; user will be warned if there is insufficient memory to run the inversion
11. Decide whether to run interactively or close the GUI and run in a batch process i.e. batch is the recommended method for all 2.5D inversions

Once the inversion has been started as a batch process then progress can be monitored by reopening the GeoModelller software and visualising progress as illustrated in the following figures.

Check the Misfit progress in the profile viewer, the Misfit % by Iteration graph or the Noise analysis graph. The Noise analysis graph shows the data by channel stripped from input data prior to inversion i.e. Signal (green), Noise (blue), IP (red negative in Z comp).

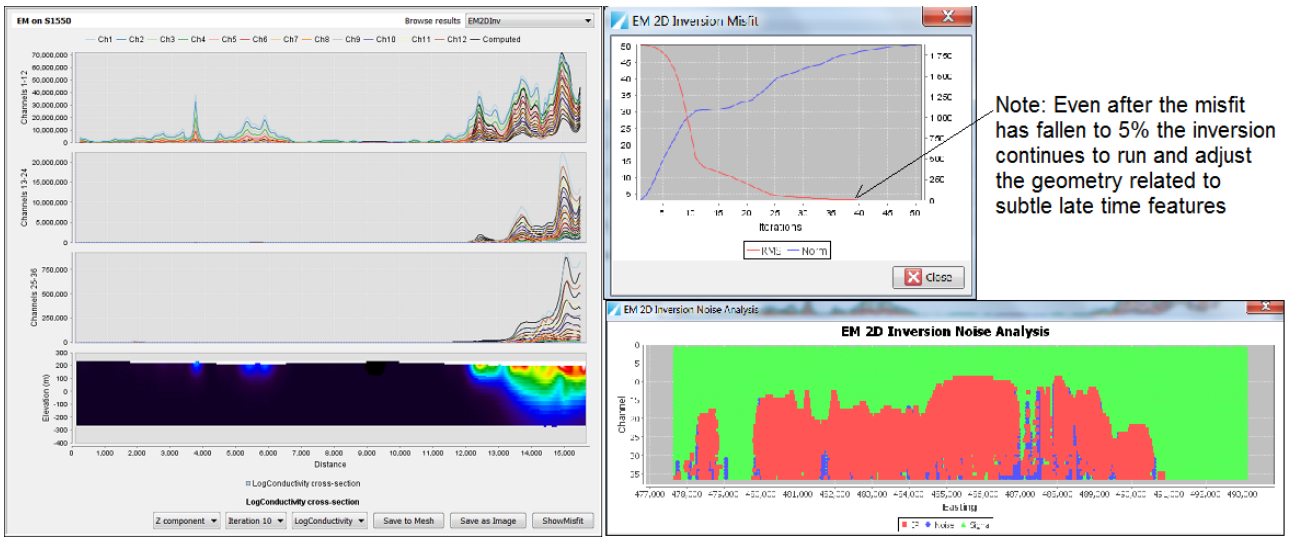

Figure 1 Clockwise from left, Misfit Profiles (Predicted in black), Misfit/Model Norm graph, Noise distribution (signal green, noise blue, IP effect red).

Once the inversion is finished, convergence has stalled or the stopping criteria are satisfied then we can visualise the inversion by iteration to perform QC. The inversion can be restarted if it has stopped too early i.e. too few iterations?

Once satisfied with the result we can transfer the final inversion to GeoModeller for 3D visualisation and analysis.

RESULTS

From the many case studies and data sets that we have worked on we present four to illustrate four different systems and geological environments. Geology for groundwater, massive sulphides, mine geology and regional mapping are easily informed by AEM using this new inversion methodology.

1. RESOLVE Riverland project, South Australia

We show a stack of 2.5D inversion log conductivity sections for a subset of lines from the RESOLVE Riverland survey highlighting in fine detail the narrow Blanchetown clay unit perched above a saline aquifer within the Parilla sands below.

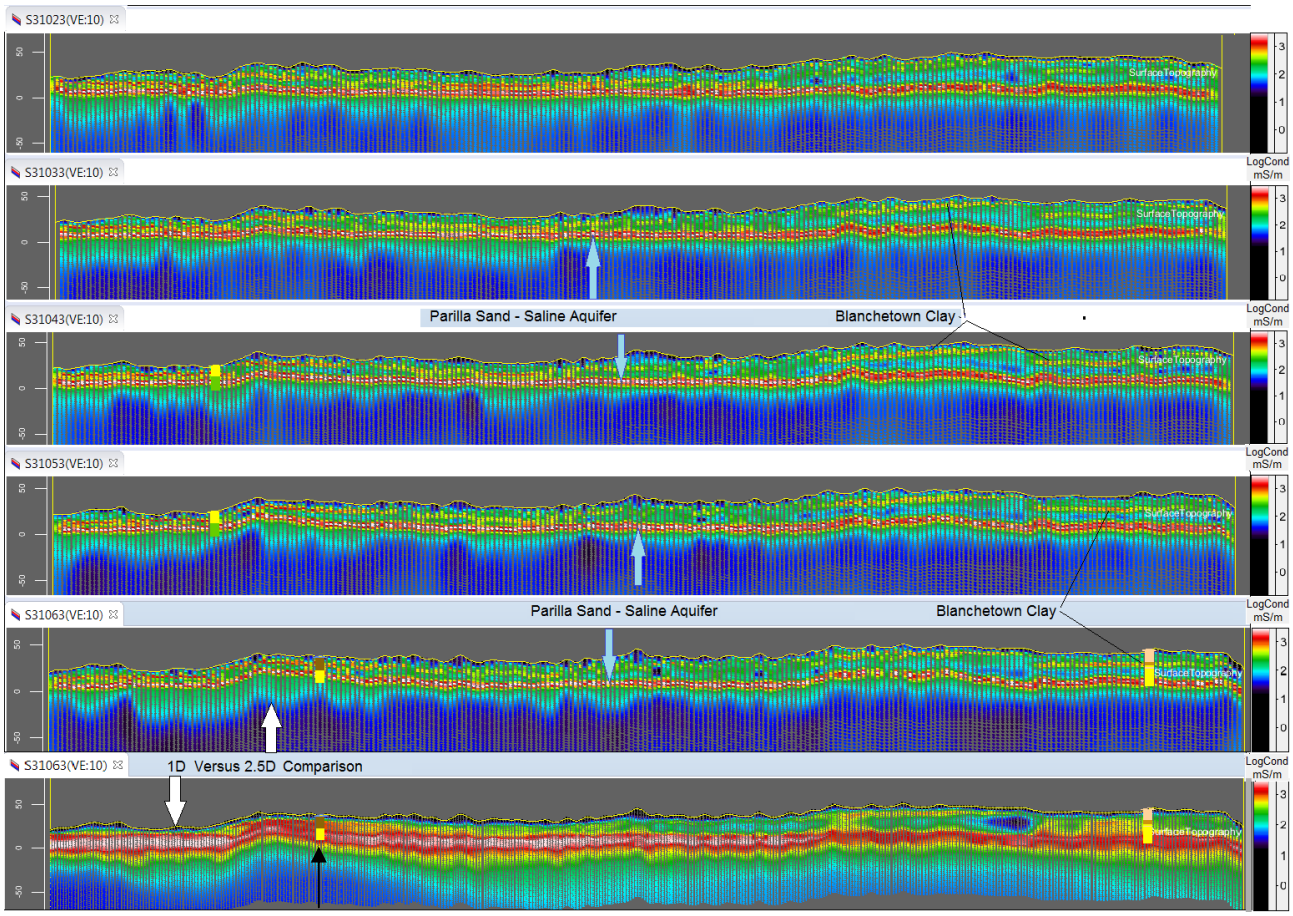

Figure 2. Resolve 2.5D Inversions defining Blanchetown Clay and Saline Aquifer compared with 1D Inversion and drilling

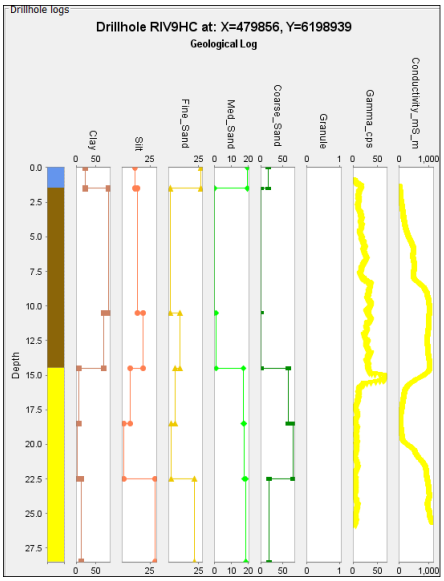

The final section in the above stack shows a 1D inversion conductivity section for Line S31063 to compare with the 2.5D inversion immediately above.

The improved definition of the clay unit and the saline aquifer in the 2.5D inversion is clearly visible.

Geology, gamma and conductivity logs for a drillhole RIV9HC (black arrow) on section S11063 are shown on the left.

2. *HELITEM*® Lalor VMS project, Manitoba, Canada

A 2.5D inversion of *HELITEM*® data south of the Lalor mine defines a large flat dipping conductivity feature 500 to 1000m below surface similar to that observed at Lalor. We examine existing drilling in the area to determine whether an ore sized target is still possible.

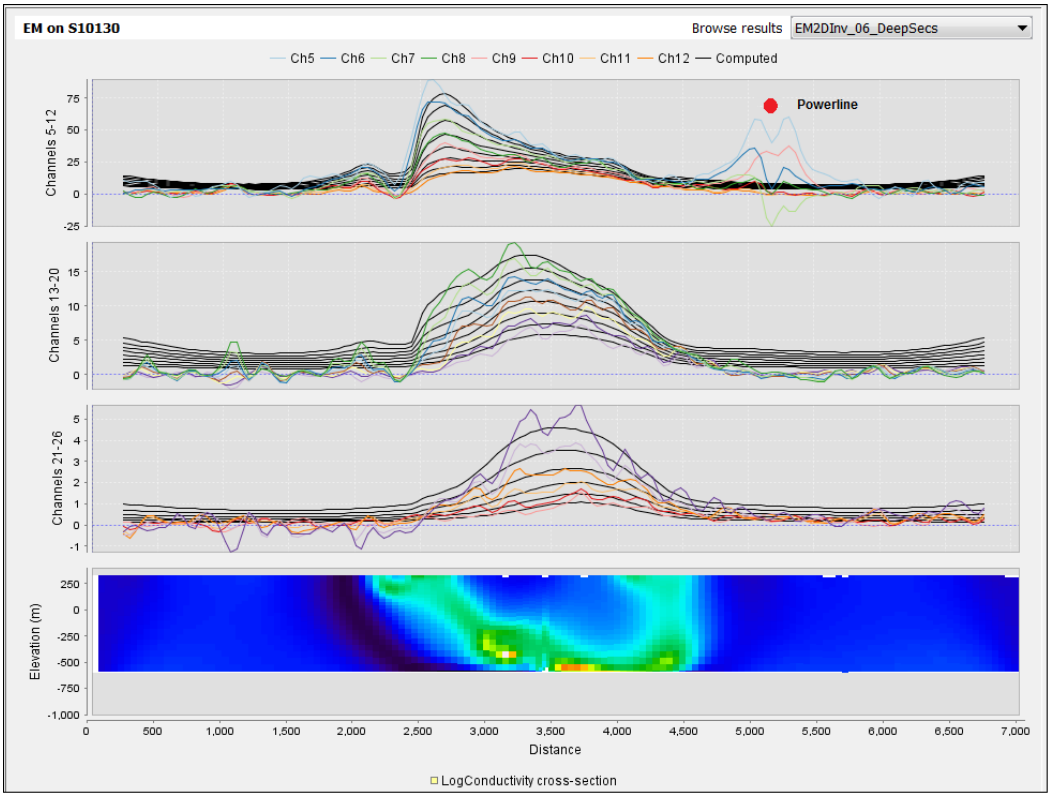

Figure 3. Measured *HELITEM*® 26 channel Z profile stack overlain with inverted profiles in black

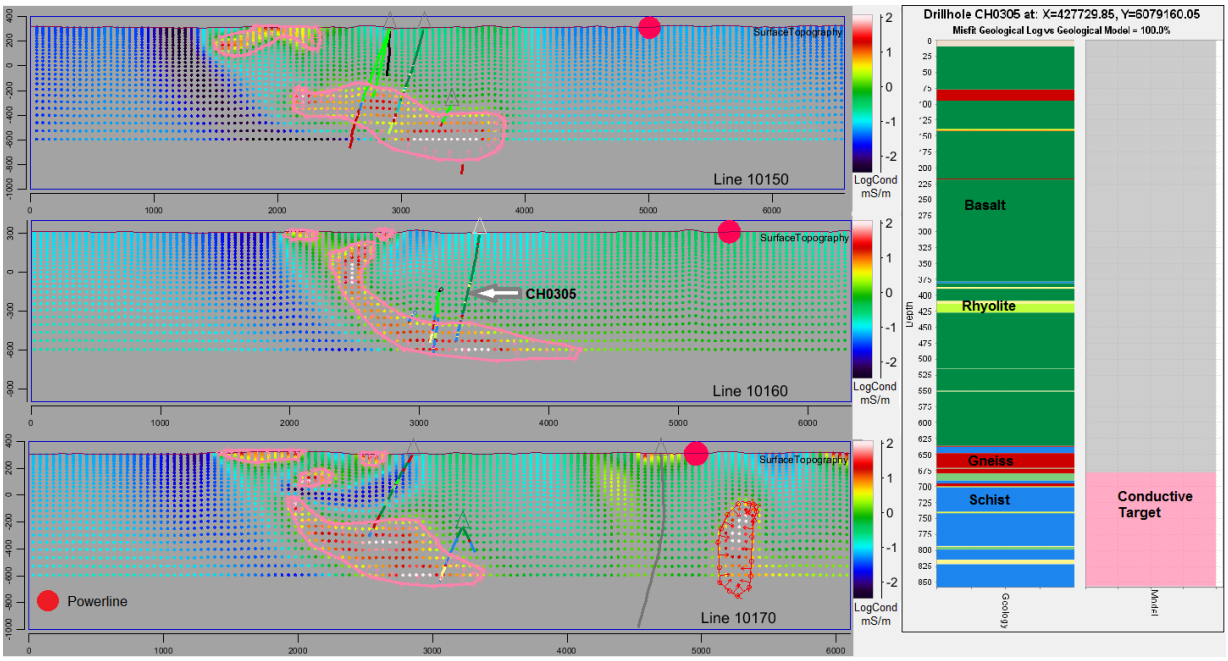

Figure 4. Conductivity Sections for Lines 10150, 10160 & 10170 with drilling and a summary log of Hole CH0305

Drilled geology suggests that the top of the broad low dipping conductive feature is related to the Hanging Wall Fault or Lalor-Chisel contact/unconformity, Caté et, 2014, below which a zone of strong alteration hosts the known VMS deposits at Lalor and Chisel Lake The conductive feature is associated with the first appearance of logged schistose and fragmental rocks in drilling i.e. CH00305.

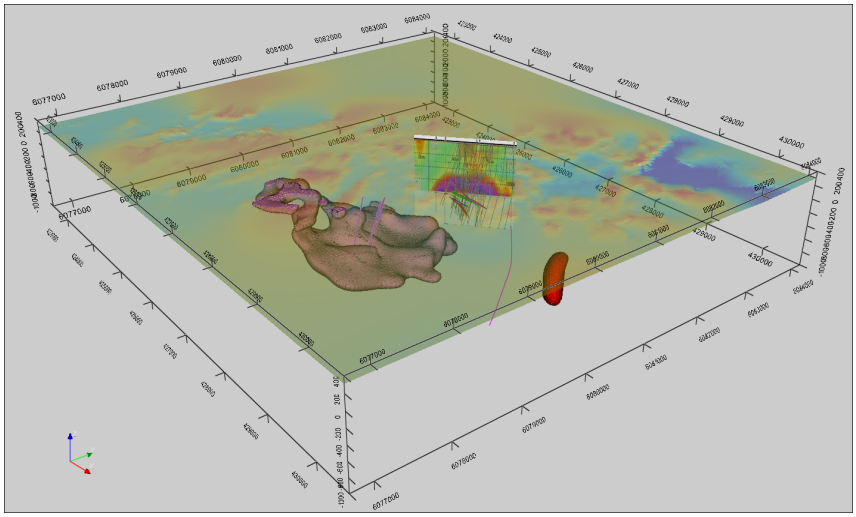

Figure 5. A 3D Perspective View of Conductive Horizon Relative to Lalor Deposit

Higher conductive zones defined by the 2.5D inversion may be targets for further accumulations of VMS style mineralisation like Lalor and Chisel Lake.

For comparison we show the UBC *HELITEM*® inversion results from Lalor section 5600N, Yang et al., 2013 in figure 6 below. The published 3D inversions show less structural detail, more coarsely defining the general Lalor deposit and alteration halo.

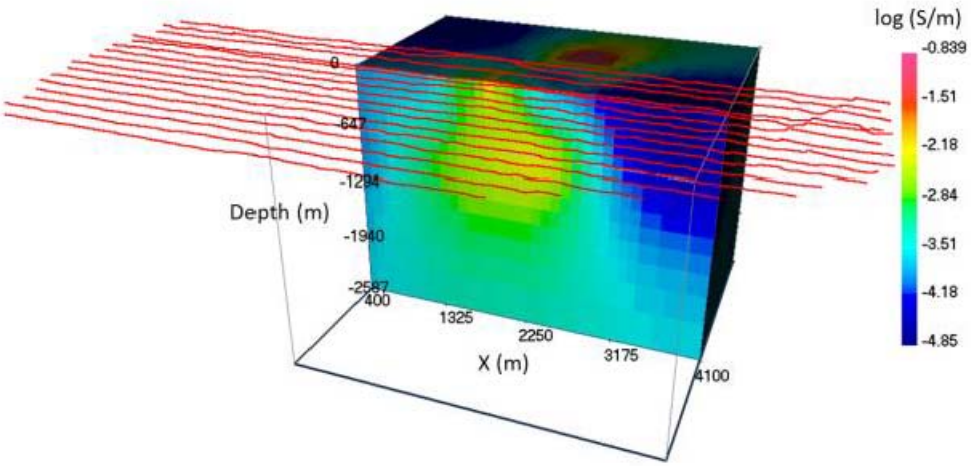

Figure 6 UBC 3D HELITEM inversion model for Lalor Lake, Yang et al., 2013

3. `Eloise VTEM™`*max* project, Cloncurry, Queensland

We illustrate a subtle late time conductive feature with near vertical geometry below a surface conductive zone. This target could be drilled without further follow up ground EM. This data also illustrates the impact of IP effects in the area.

In Figure 7 we show a single target conductor on Line 1560 illustrating the inverted profiles in black over the 36 channel observed VTEM. The Misfit graph in % and the Noise and IP effect along line stripping map. 2.5D Inversion misfits in this survey are excellent at ~5%. The **`VTEM™`*max*** system generates strong IP effects along the majority of lines in this study and these appear to be generated by near surface clays. Note that IP effects are removed from the observed signal prior to inversion for VTEM and other symmetric loop systems.

We show the results of drilling on flight line 1590 towards the south after follow-up of the VTEM survey with moving loop ground EM, Thompson, A., 2016 (pers comm).

The conductive target is shown on seven flight lines in Figure 8 below together with the drill log for the tested target on Line 1590. The source of the anomaly is graphitic shale.

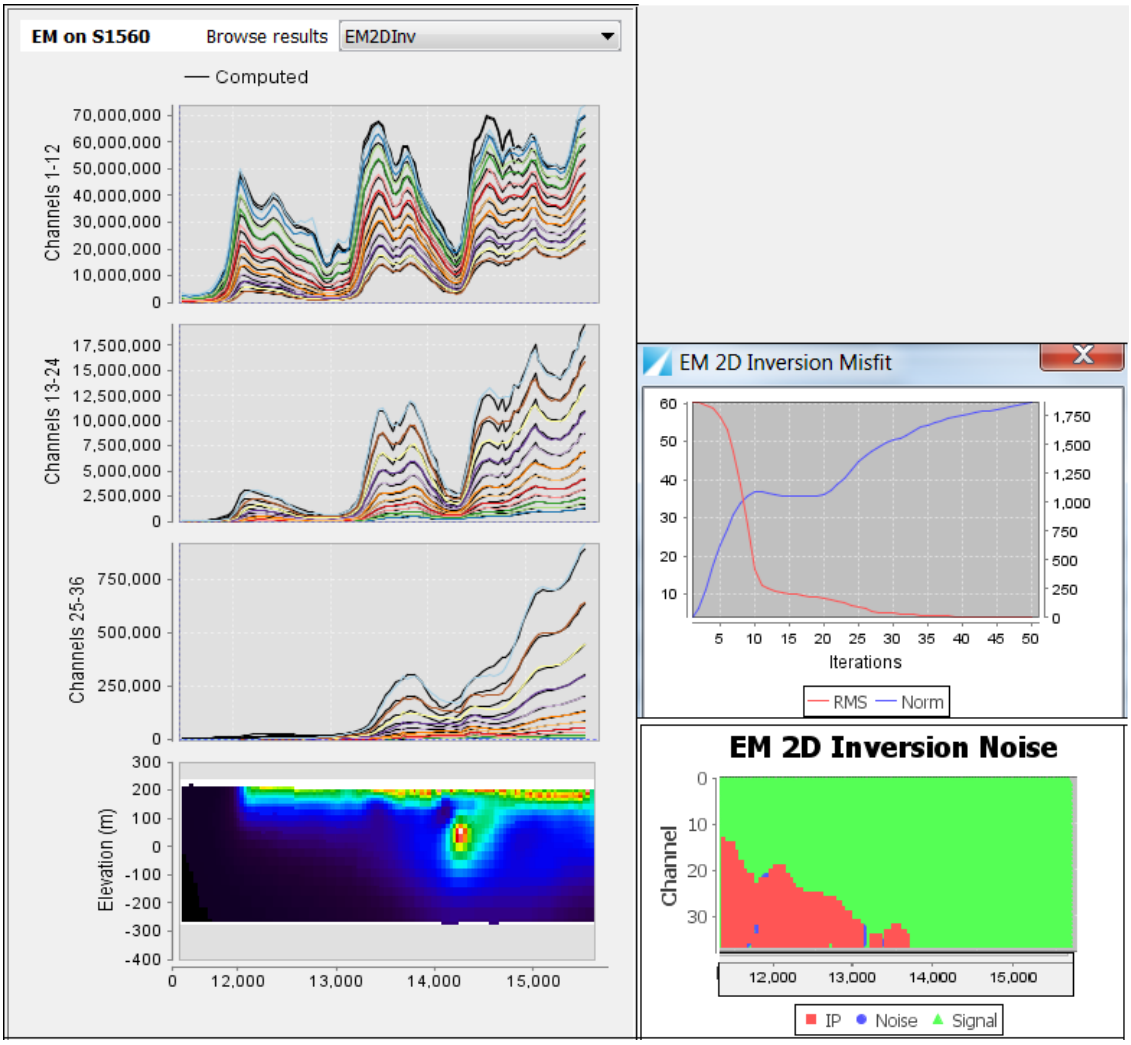

Figure 7. Target Conductor Line 1560, Misfit Graph and Stripped Noise Map

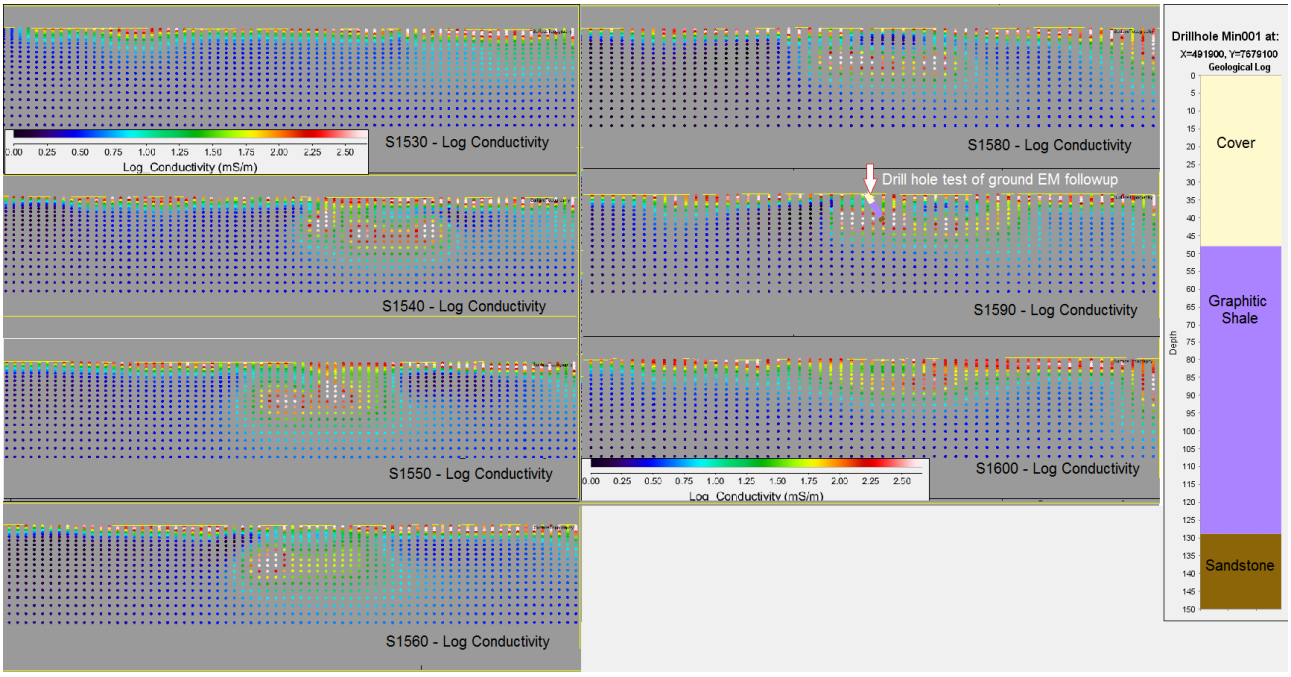

Figure 8. Log Conductivity Section Stack - 7 Lines

4. TEMPEST Tarcoola Area 6 project, Marmota Energy, Wadikee, South Australia

Another subtle late time target below conductive cover clearly identified in the 2.5D, Z and joint XZ inversions. Only Z component is shown here.

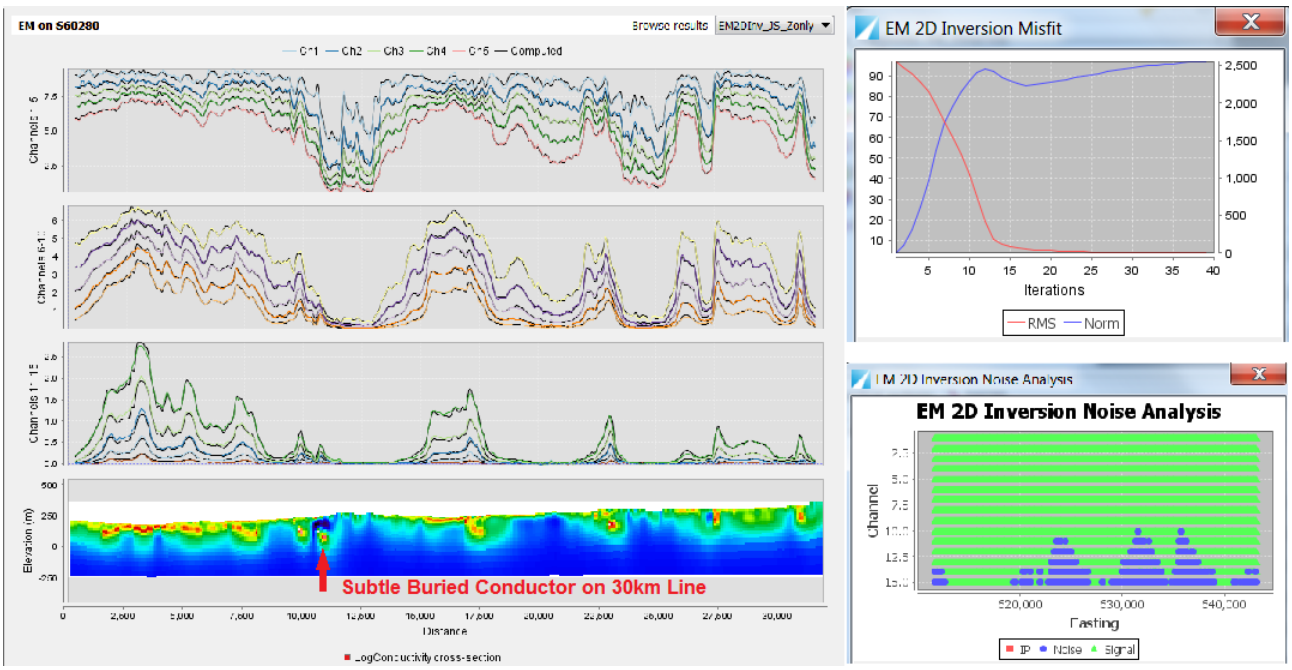

Figure 9. Tarcoola Tempest Line showing clockwise from left, small conductive target beneath conductive cover, Misfit (~5%) top right and Stripped Noise map.

CONCLUSIONS

The examples presented show the ability of this 2.5D inversion application to resolve the geometry of subtle late time and deep conductivity features when compared with more commonly used CDI transforms, simple 1D inversions or relatively low resolution smooth 3D inversions.

The results in these examples have been obtained in a blind inversion sense using a simple half space starting model and a 1000 ohm-m starting resistivity. There has been no attempt made to bias the results using a reference model derived from a priori knowledge of the survey area. We contend that creating geological sections from these inversions will add a lot to the geology model building process.

Resolution of geology to depths of >1km are demonstrated where AEM system power and conductivity distribution allow as in the Lalor case.

Engineering to reduce memory and increase performance by use of the INTEL Pardiso solver, INTEL MPI parallelisation and optimisation of the sensitivity matrix enables data from survey lines with lengths exceeding 30 kilometres to be inverted on a high end laptop computer.

A new simplified tool to manage the complexity of AEM can be placed in the hands of the non-specialist.

ACKNOWLEDGMENTS

The authors wish to thank CGG for providing the *HELITEM*® survey data from Lalor and Hudbay Minerals Inc. for providing helpful comments and some relevant drillhole geological data.
We also wish to thank Minotaur Exploration Ltd for providing their VTEM™ *max* survey data and permission to publish results.

REFERENCES

Brodie, R.C., Green A.A., and Munday, T.J., 2003. Constrained inversion of RESOLVE airborne electromagnetic data, Riverland and Tintinara East, South Australia: Data calibration report. CRCLEME Restricted Report 190R.

Brodie, R.C., Green A.A., and Munday, T.J., September 2004. Constrained inversion of RESOLVE airborne electromagnetic data, Riverland, South Australia CRC LEME OPEN FILE REPORT 175.

Carter, R., Schwartz, T., West, S., Hoover, K., Lalor Concentrator Project, Hudbay.Pre-Feasibility Study Technical Report, on the Lalor Deposit, Snow Lake, Manitoba, Canada Effective Date: March 29th, 2012

Calcagno, P., Chilès, J, P., Courrioux, G., Guillen, A., 2008, Geological modelling from field data and geological knowledge Part I. Modelling method coupling 3D potential - field interpolation and geological rules, 'Physics of the Earth and Planetary Interiors' 171 (2008) 147 – 157

Caté, A., Mercier-Langevin, P., Ross, P.S. and Simms, D., 2014, Structural controls on geometry and ore distribution in the Lalor auriferous VMS deposit, Snow Lake, west-central Manitoba (part of NTS 63K16): preliminary results from underground mapping; in Report of Activities 2014, Manitoba Mineral Resources, Manitoba Geological Survey, p. 104–115.

Guillen, A., Calcagno, P., Courrioux, G., Joly, A., Ledru, P., 2008, Geological modelling from field data and geological knowledge Part II. Modelling validation using gravity and magnetic data inversion, Physics of the Earth and Planetary Interiors 171 (2008) 158 - 169

Hayley K., Silic J., FitzGerald D., Paterson R., (2016), Quantitative assessment of the value added to regional groundwater model predictions by airborne electromagnetic surveys, KEGS 2016 PDAC Symposium, Geophysics and the Environment, 2016.

Hodges, G., Chen, T., van Buren, R., 2015, HELITEM Detects the Lalor Deposit, SAGA 2015 Abstracts, 14th Biennial Geophysical Conference, Drakensburg, South Africa.

Hodges, G., Chen, T., 2014, Lalor HeliTEM Test Results, Proceedings from Exploration for Deep VMS Ore Bodies: The HudBay Lalor Case Study, British Columbia Geophysical Society 2014 Fall Symposium.

Munday, Timothy , Ley Cooper, Yusen , Johnson, Simon , Tyler, Ian (2013), A regional scale fixed-wing TDEM surey of the Palaeo-Proterozoic Bryah Basin, Western Australia: Providing insights into a geological setting highly prospective for VMS Cu-Au and mesothermal Au Systems. ASEG Extended Abstracts 2013 , 1–4.

Silic J., Paterson R., FitzGerald D., Archer T., (2015), Comparing 1D and 2.5D AEM inversions in 3D geological mapping using a new inversion solver. 14th International Congress of the Brazilian Geophysical Society , Extended Abstracts.

Taylor, C., 2014, Mine scale description of the mineralization at the Lalor deposit, Snow Lake, Manitoba, Canada: Proceedings from Exploration for Deep VMS Ore Bodies: The HudBay Lalor Case Study, British Columbia Geophysical Society 2014 Fall Symposium, 1–3.

Wilson, G.A., Raiche, A.P. & Sugeng, F., 2006, 2.5D inversion of airborne electromagnetic data. Expl. Geoph., 37, 363-371.

Yang, D., and Oldenburg, D. W., 2013, 3D conductivity model of the Lalor Lake VMS deposit using ground and airborne EM data: ASEG Extended Abstracts 2013, 23rd Geophysical Conference: Australian Society of Exploration Geophysicists, 1–4.